International Journal of Engineering

Development of a Non-Iterative Macromodeling Technique by Data Integration and Least Square Method

M. Sedaghat[a], Z. H. Firouzeh[*a], H. Aliakbarian[b]

[a] Department of Electrical and Computer Engineering, Isfahan University of Technology, Isfahan, Iran
[b] Department of Electrical Engineering, KN Toosi University of Technology, Tehran, Iran

PAPER INFO	ABSTRACT
	In this paper, a new method is introduced to synthesize the original data obtained from simulation or measurement results in the form of a rational function. The integration of the available data is vital to the performance of the proposed method. The values of poles and residues of the rational model are determined by solving the system of linear equations using conventional Least Square Method (LSM). To ensure the stability condition of the provided model, a controller coefficient is considered. Also, using this parameter, the designer can increase the stability margin of a system with poor stability conditions. The introduced method has the potential to be used for a wide range of practical applications since there is no specific restriction on the use of this method. The only requirement that should be considered is Dirichlet condition for the original data, usually the case for physical systems. To verify the performances of the proposed method, several application test cases were investigated and the obtained results were compared with those gathered by the well-known vector fitting algorithm. Also, the examinations showed that the method is efficient in the presence of noisy data.

1. INTRODUCTION

Full detail modeling of many practical structures in engineering fields, such as solving Maxwell's equations at the system level, is very difficult based on the first principle [1]. This is because the complete simulation of these structures is highly time-consuming and needs a large amount of memory [2, 3]. In some cases, the complexity is due to the electrical size of the structure leading to an unreasonable number of unknowns. Especially with increasing frequency, fully detailed analysis has become the main requirement for all state-of-the-art circuit design and simulations [4, 5]. Furthermore, simulators face trouble in simulating the structures in the presence of nonlinear components due to mixed frequency/time problems as well as CPU inefficiency [6, 7]. It is well-known that characteristics of understudying structures are governed by Telegrapher's equations of Partial Differential Equations (PDEs) considered to be best solved in the frequency domain, while nonlinear elements are described in the time

domain using Ordinary Differential Equations (ODEs) [8-9]. The mentioned problems could be observed in various cases such as on-chip, packaging structures, power systems, printed circuit boards (PCB) and etc. In such situations, a common technique is to divide this complexity into two cases. In the first case, physical characteristics of the structure are known and modeling is based on the most appropriate method. In the second case, where a physical structure is unknown or any analytic solution is hard to derive, rational macromodeling approximation from full-wave electromagnetic simulation or port-port measured data are used to the model system [7].

Several types of black-box macromodeling are done using known physical characteristics of the system [10]. These models are established following many different methods, depending on the available data from the understudying system [11]. These methods lead to three general flows including macromodeling via model order reduction, macromodeling from field solver data, and macromodeling from measured responses. Also, rational

*Corresponding Author Institutional Email: zhfirouzeh@iut.ac.ir (Z. H. Firouzeh)

approximation modeling can be constructed from tabulated data responses, as it may also be obtained by a full-wave simulation or through measured data in the frequency domain often existing in the form of impedance, hybrid, scattering, or admittance parameters data. To this end, several methods are proposed, including Vector Fitting (VF) algorithm [12, 13], brute force lumped segmentation modeling [14], the Loewner framework [15, 16], Passive Reduced-Order Interconnect Macromodeling Algorithm (PRIMA) [17], Matrix Rational Approximation (MRA) [18, 19], compact difference [20], integral congruent transformation [21, 22] and so on.

In terms of efficacy, accuracy, and complexity, all the above mentioned methods have their own advantages and disadvantages. For example, vector fitting is currently one of the most popular pole-residue based system identification tools formulated as a linear least-squares problem, depending on an iterative pole relocation approach to improve the approximation. Some advantages to this algorithm include high computational efficiency, high model accuracy, and a relatively simple formulation. Unlike vector fitting, Loewner Method is very efficient in identifying the system from the tabulated data with fewer state-space equations [15, 23]. In Loewner Matrix modeling, the order of the system could be identified from the Singular Value Decomposition (SVD) of Loewner Matrix [23].

In this work, a mathematical method for developing a rational-based transfer function model for practical applications is introduced; addressing the challenges of low complexity. This method is developed based on the integration of the original simulated or measurement data at several specified intervals to decrease data losses and increase the accuracy of the final outcome. For the number of integration intervals, a number of equations are obtained. The result is a system of linear equations. Then, using the Least Square Method (LSM), the required values, including poles and residues of the rational form of the model are determined. To ensure the stability condition of the final response, a closed-loop model is attributed to the understudying system. This goal will be met through defining a stability controller coefficient for the closed-loop model. Several practical examples are provided to evaluate the performance of the proposed method. We tried herein to first present the mathematical formulation of the proposed method in section 2. Then to investigate several examples and comparing the obtained results of the vector fitting algorithm in section 3. Finally, reaching a conclusion in section 4.

2. MATHEMATICAL FORMULATION

Practical structures are modeled using simulation or measured data from frequency-dependent scattering,

impedance, or admittance parameters. It is common to acquire a rational function to approximate the obtained data as follows [1].

$$H(x) = \sum_{n=1}^{N} \frac{r_n}{x - p_n} + r_0 \tag{1}$$

where r_n, p_n correspond to residues and poles respectively, while the value r_0 is optional; x can be considered as frequency f or Laplace variable s (complex frequency), and N is the number of poles and residues or the order of the rational function. The other common notation of rational transfer functions $H(x)$ is described as the ratio of two polynomials

$$H(x) = \frac{P(x)}{Q(x)} = \frac{b_{N_P} x^{N_P} + b_{N_P-1} x^{N_P-1} + \ldots + b_1 x + b_0}{a_{N_Q} x^{N_Q} + a_{N_Q-1} x^{N_Q-1} + \ldots + a_1 x + 1} \tag{2}$$

In which, the degree of the prescribed numerator and denominator polynomials $P(x)$ and $Q(x)$ are N_P and N_Q, respectively. In most cases, it is assumed that $N_P = N_Q = N$. One of the simplest assumptions in the underlying model structure is using the linear least square method. Multiplying by $Q(x)$ both sides of equation (2) and some simplification leads to:

$$\begin{aligned} b_0 + b_1 x - a_1 H(x) x + b_2 x^2 - a_2 H(x) x^2 \\ + \ldots + b_n x^N - a_n H(x) x^N = H(x) \end{aligned} \tag{3}$$

Samples of the desired transfer function at each $x = x_m$; $m = 1, 2, \ldots, M$ are available. Using these samples, the above equation can be rewritten as a linear system of M equations in $2N+1$ unknown, where M is the total number of samples [1].

$$\boldsymbol{\Phi u} = \mathbf{v} \tag{4}$$

$$\boldsymbol{u} = [b_0 \quad \cdots \quad b_N \quad a_1 \quad \cdots \quad a_N]^T \tag{5a}$$

$$\boldsymbol{v} = [H(x_1) \quad H(x_2) \quad \cdots \quad H(x_M)]^T \tag{5b}$$

$$\boldsymbol{\Phi} = \begin{bmatrix} 1 & \cdots & x_1^N & -x_1 H(x_1) & \cdots & -x_1^N H(x_1) \\ \vdots & & & \ddots & & \vdots \\ 1 & \cdots & x_M^N & -x_M H(x_M) & \cdots & -x_M^N H(x_M) \end{bmatrix} \tag{5c}$$

It is assumed that coefficient matrix $\boldsymbol{\phi}$ is not a zero matrix. Typically, equations number M is greater than the unknown number $2N+1$. Therefore, by assuming that the coefficient matrix is left-invertible, the following equation is the unique solution to the least-squares problem (4) [24].

$$\tilde{u} = (\boldsymbol{\Phi}^T \boldsymbol{\Phi})^{-1} \boldsymbol{\Phi}^T \boldsymbol{v} \tag{6}$$

It is clear that the above solution is not an exact answer for any choice of $\mathbf{u}$. The solution defined by (6) is the vector that minimizes the sum of squares of the error vector $\mathbf{E}$ defined as the Euclidean norm as follows [25].

$$\boldsymbol{E} = \|\boldsymbol{\Phi} \tilde{u} - \boldsymbol{v}\|^2 \tag{7}$$

This method is affected by several issues. First, the coefficient matrix $\boldsymbol{\phi}$ known as the Vandermond matrix,

becomes seriously ill-conditioned when order of numerator and/or denominator polynomials increases. Second, solution (6) will be successful, whereas there is a linear relationship between variable x and the desired transfer function $H(x)$. However, in practical applications, this condition is not provided [25, 26]. Furthermore, this method suffers from local control over the unshaped area of the desired data [27]. In other words, in this method, information between two adjacent samples is not used. If the goal is to use all the information, the number of unknowns, being the degree of the numerator and the denominator polynomials of (2), increases dramatically. This problem could be solved by integrating both sides of the equation (3) over an interval $[x_i, x_f]$.

$$\int \{b_0 + b_1 x - a_1 H(x)x + b_2 x^2\}dx +$$
$$\int \{-a_2 H(x)x^2 + \dots + b_n x^N - a_n H(x)x^N\}dx = \quad (8)$$
$$\int H(x)\,dx$$

Some simplifications could also be made as follows.

$$b_0 x + \frac{b_1}{2}x^2 + \dots + \frac{b_n}{N+1}x^{N+1} - a_1 \int H(x)x\,dx -$$
$$a_2 \int H(x)x^2 dx \dots - a_n \int H(x)x^N dx = \int H(x)dx \quad (9)$$

For a given desired data, the integration result for both left and right-hand sides of the above equation could be calculated. The unknown numbers are $2N+1$. Hence, at least $2N+1$ independent equations are required. In practical application, it is assumed that the desired data are available from frequency interval $f \in [f_{min}, f_{max}]$. As mentioned before, x could be considered as a frequency f or Laplace variable s. Hence, x is varying over the interval $x \in [x_{min}, x_{max}]$, where x_{min} and x_{max} correspond to a minimum and maximum frequency, respectively. By dividing the distance $x_{min} \le x \le x_{max}$ to M equal segments, the required number of equations will be obtained.

$$x \begin{cases} x1_{min} \\ xM + 1_{max} \end{cases} \Big| \xrightarrow{\text{Integ. Interval}} x\,m + 1 \;\; {}_m max_{min} \quad (10)$$

By specifying upper and lower limits of the integration interval, only the coefficient's a_i, b_i remains unknown. As a result, a linear system of M equations and $2N+1$ unknown is made. This equation system and its solution are as follows.

$$\boldsymbol{\Psi u} = \boldsymbol{w} \quad (11a)$$

$$\tilde{\boldsymbol{u}} = (\boldsymbol{\Psi^T \Psi})^{-1}\boldsymbol{\Psi^T w} \quad (11b)$$

where $\boldsymbol{\Psi}$ is $M \times 2N+1$ coefficient matrix, $\mathbf{u}$ is $2N+1 \times 1$ column vectors, in which holds the unknowns, and $\mathbf{w}$ is $M \times 1$ column vectors that include the desired data.

$$\boldsymbol{u} = [b_0 \;\; \cdots \;\; b_N \;\; a_1 \;\; \cdots \;\; a_N]^T \quad (12a)$$

$$\boldsymbol{w} = \left[\int_{x_1}^{x_2} H(x)dx \;\; \cdots \;\; \int_{x_M}^{x_{M+1}} H(x)dx\right]^T \quad (12b)$$

$$\boldsymbol{\Psi} = \begin{bmatrix} \int_{x_1}^{x_2} dx & \cdots & \int_{x_1}^{x_2} x^N dx & -\int_{x_1}^{x_2} xH(x)dx & \cdots & -\int_{x_1}^{x_2} x^N H(x)dx \\ \vdots & & \ddots & & & \vdots \\ \int_{x_M}^{x_{M+1}} dx & \cdots & \int_{x_1}^{x_2} x^N dx & -\int_{x_1}^{x_2} xH(x)dx & \cdots & -\int_{x_M}^{x_{M+1}} x^N H(x)dx \end{bmatrix} \quad (12c)$$

In some practical cases, using equation (11b) is not a good solution, especially when $\boldsymbol{\Psi}$ is an ill-conditioned matrix, and it may cause a low accuracy in the final answer. In these cases, using of a modified QR factorization technique leads to an increase in computational efficiency, where $\mathbf{P}$ is the permutation matrix [1].

$$\tilde{\boldsymbol{u}} = \boldsymbol{PR^{-1}Q^T w} \quad (13a)$$

$$\boldsymbol{\Psi P} = \boldsymbol{QR} \quad (13b)$$

It could be seen that the integral responses in Equation (12) are independent of variable x. This ensures that the proposed method is less affected by any unwanted noise or disturbance. In other words, the integral operator is resistant to noise. As mentioned before, the typical least square method suffers from a nonlinear feature understudying systems while the integral operator solves this problem. In many former researches in literature, they use only samples of the available data. This means that, in these methods, all observable output of the system is not used properly and there is a data loss problem, while in the proposed technique, all available data are used in the integration process, and there is not any data loss.

According to equation (12), three conditions should be met. First, available data should be absolutely integrable over any interval. Second, available data should be of bounded variation in any given bounded interval. Third, available data should have a finite number of discontinuities in any given bounded interval, and the discontinuities cannot be infinite. In summary, Dirichlet condition should be met as follows [28].

$$\int_x |H(x)|dx < \infty \quad (14a)$$

$$\int_x |H(x)x^n|dx < \infty; \; n \text{ is integer} \quad (14b)$$

The computational complexity of Equation (11) is dependent on the value of M. The Nyquist theorem can be helpful to determine the sampling rate Δ. For an arbitrary available data, the following equation can be used to the first approximation of M [26].

$$\Delta \le \frac{|x_{max} - x_{min}|}{4N} \quad (15a)$$

$$M \ge \frac{8N}{|xmin_{max}|} \quad (15b)$$

In other words, the number of integration intervals is

considered equal to the number of samples. It should be noted that the above equations are obtained, assuming that the integration intervals have equal lengths. In some cases, intervals of equal length may not produce acceptable results. For these cases, the number of integral intervals of a range of x that are more important could be increased. Correspondingly, for regions of x that the original data is less important, less number of integral intervals could be considered. For example, if the original data is the frequency response of a bandpass filter, the number of integral intervals in the passband range will be considered greater than the number of integral intervals in the stopband range.

After determining the unknown coefficients a_i, b_i using Equation (11), poles, and zeros of Equation (2) should be determined. The poles and zeros are Eigen-values of the following matrixes [29].

$$T_P = \begin{bmatrix} -\frac{b_{N-1}}{b_N} & -\frac{b_{N-2}}{b_N} & \cdots & -\frac{b_0}{b_N} \\ 1 & 0 & \cdots & 0 \\ \vdots & \ddots & & \vdots \\ 0 & 0 & 1 & 0 \end{bmatrix}_{N \times N} \tag{16a}$$

$$T_Q = \begin{bmatrix} -\frac{a_{N-1}}{a_N} & -\frac{a_{N-2}}{a_N} & \cdots & -\frac{1}{a_N} \\ 1 & 0 & \cdots & 0 \\ \vdots & \ddots & & \vdots \\ 0 & 0 & 1 & 0 \end{bmatrix}_{N \times N} \tag{16b}$$

By specifying the poles and zeros of the system, available data could be expressed in poles-residues form as (1). As mentioned before, in physical problems, x is some independent variable such as real frequency f or complex frequency s in order of GHz. To avoid the computational complexity, before incoming the process, variable x can be normalized to its maximum value. After specifying the poles and residue, the rational form can be easily rescaled to its normal case.

In some cases, the obtained poles may be placed in an unstable region. In the following, a simple technique will be introduced to overcome this problem. The general form of a closed-loop system with forward transfer function $G(x)$ and feedback transfer function $F(x)$ is presented in Figure 1. The transfer function of the closed-loop system is as follows.
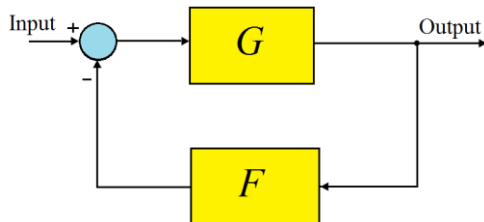
$$TF(x) = \frac{G(x)}{1+G(x)F(x)} \tag{17}$$

Figure 1. Block diagram of a closed-loop system

For simplicity, it is assumed that the feedback transfer function is equal to one and the forward transfer function could be expressed as a ratio of two polynomials. This system is considered as a macromodel to the understudying system as follows.

$$TF(x) = \frac{G(x)}{1+G(x)F(x)} \xrightarrow{F(x)=1\,G(x)=k\frac{B(x)}{A(x)}}$$
$$TF(x) = \frac{kB(x)}{A(x)+kB(x)} \tag{18}$$

Therein, parameter k is a stability controller coefficient, using which the stability of the model could be controlled. By comparing Equation (18) with Equation (2), we have:

$$H(x) = \frac{kB(x)}{A(x)+kB(x)} = \frac{kB(x)}{C(x)} =$$
$$k\frac{b_N x^N + b_{N-1}x^{N-1}+\ldots+b_1 x+b_0}{c_N x^N + c_{N-1}x^{N-1}+\ldots+c_1 x+c_0} \tag{19a}$$

$$\begin{cases} c_n = a_n + kb_n \\ c_0 = 1 + kb_0 \end{cases}, n = 1,2,\ldots,N \tag{19b}$$

In this situation, the proposed procedure is applied to a new case. In other words, Equation (12c) should be rewritten for a new case.

$$\Psi = [\Psi_b \quad \Psi_a] \tag{20a}$$

$$\Psi_b = k \begin{bmatrix} \int_{x_1}^{x_2} h(x)dx & \cdots & \int_{x_1}^{x_2} h(x)x^N dx \\ \vdots & \ddots & \vdots \\ \int_{x_M}^{x_{M+1}} h(x)dx & \cdots & \int_{x_M}^{x_{M+1}} h(x)x^N dx \end{bmatrix} \tag{20b}$$

$$\Psi_a = \begin{bmatrix} -\int_{x_1}^{x_2} xH(x)dx & \cdots & -\int_{x_1}^{x_2} x^N H(x)dx \\ \vdots & \ddots & \vdots \\ -\int_{x_M}^{x_{M+1}} xH(x)dx & \cdots & -\int_{x_M}^{x_{M+1}} x^N H(x)dx \end{bmatrix} \tag{20c}$$

$$h(x) = 1 - H(x) \tag{20d}$$

As a result, by changing the parameter k, the stability condition could be met. In other words, unstable poles could be moved toward the stable region. Another solution is to plot the root locus of the system and determining the acceptable value of k that guarantees the stability condition.

Passivity can be achieved through the conventional two-step methods introduced in literature [1]. In this way, first step comprises of approximation with stable poles. Then, using the method of repetition and perturbation in the residues, we can achieve the condition of being passive. More details are available in literature [1]. Also, the proposed method could be easily extended for Multi-Input-Multi-Output systems (MIMO) using the introduced procedure by Grivet-Talocia et al. [1].

3. RESULTS AND DISCUSSIONS

In this section, the performance of the proposed method will be demonstrated using several examples. It should be noted that the purpose of this paper is not to show the

overall superiority of the proposed method over the VF algorithm; although, this is obvious in some examples. Here, the realxed VF algorithm version 3 is used as a known method to compare the results [31].

3. 1. Single Trace PCB   A single trace PCB, as shown in Figure 2 with a length of 10 cm is considered as the first example. The width of the strip and substrate height is about 1.55 mm, 0.8 mm, respectively. The applied substrate is FR4 with a relative permittivity of 4.3. This structure is simulated using CST microwave studio in time domain. The corresponding scattering parameters ranged between 0 and 5 GHz are considered as the input of the problem. The magnitude and phase of rational approximation of S21 using the proposed method with 6 poles (N=6) and vector fitting algorithm with N=8, 10 poles for the first example are shown in Figures (3a) and (3b). It can be seen that VF with N=8 shows a small deviation in magnitude, but by increasing the poles number to N=10, the synthesized error is decreased. A comparison of the results shows that the proposed method has a better performance with a lower number of poles.

3. 2. MultiLayer Structure   The second example is a multilayer structure shown in Figure 4. In this structure, a microstrip trace with width and length of 1.18 mm, 8.49 mm, respectively, in signal layer is connected to a stripline trace in the third layer with width and length 0.47 mm, 22.64 mm, respectively. The copper planes in layers 2 and 4 are regarded as ground. A FR4 substrate
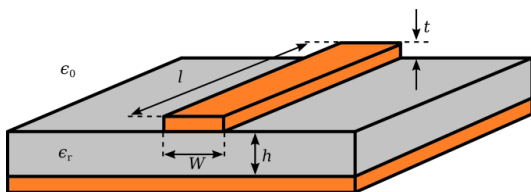

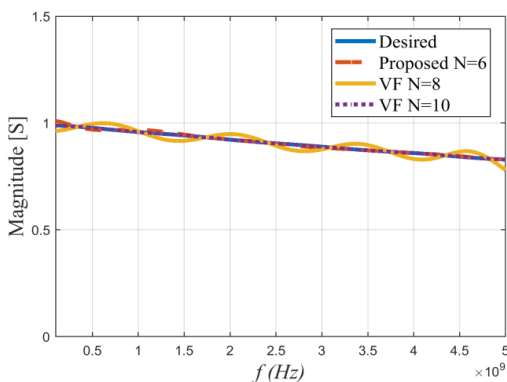**Figure 2.** The geometry of a single trace PCB

Figure 3a. Magnitude of the synthesized S_{21} of single trace PCB
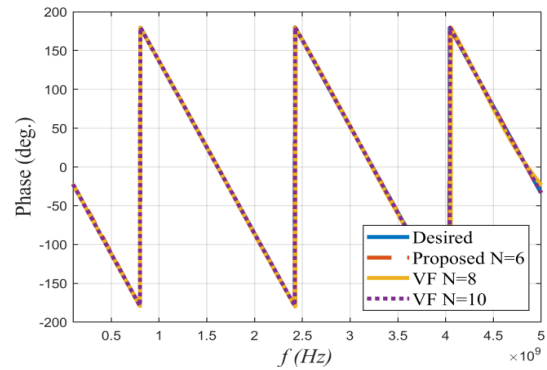

Figure 3b. Magnitude of the synthesized S_{21} of single trace PCB

with relative permittivity, loss tangent and height 4.3, 0.02 and 0.6 mm, is used for this example. The structure is terminated matched load (50 Ohms impedance). The simulated scattering parameters in frequency ranged from 0 to 5GHz are considered as the available data to the synthesis procedure. Figure 5 shows the rational approximation results of the example for the proposed method with two different poles numbers N=3, 8 and vector fitting algorithm with N=6. Although the vector fitting algorithm and the proposed method with N=8 have an acceptable accuracy, the VF was able to synthesize the problem with a smaller number of poles.
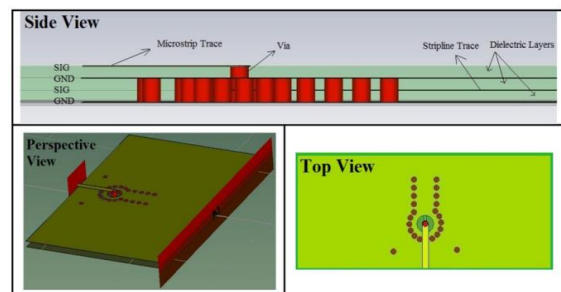

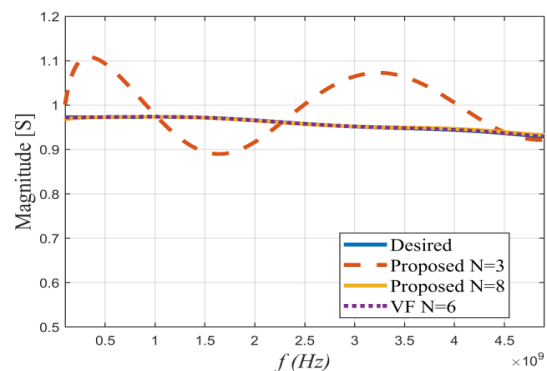**Figure 4.** The structure geometry of multilayer microstrip

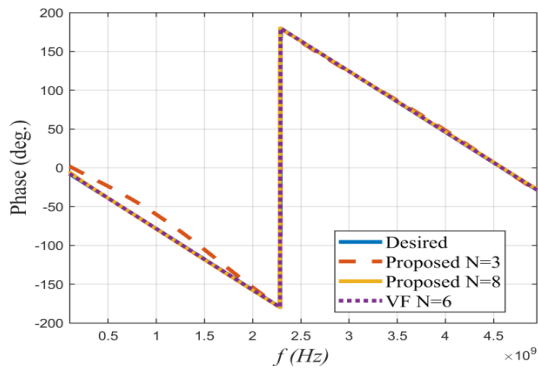**Figure 5a.** Magnitude of synthesized S_{21} of multilayer microstrip

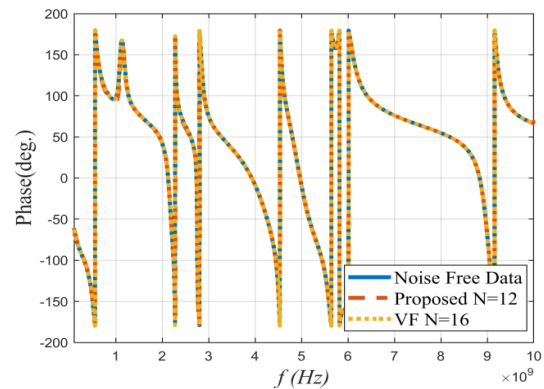**Figure 5b.** Phase of synthesized S_{21} of multilayer microstrip

3. 3. Noise-Infected Data   The third test case is a theoretical example in which the goal is to assess the performance of the proposed method for noise-infected data in frequency ranged from 0 to 10 GHz. This example includes a synthetic transfer function with 16 poles described in Table 1 [30]. First, the synthetic transfer function is considered to be noise-free. Figure 6 shows the obtained results of the proposed method with N=12 and VF algorithm with *N*=16. The performance of the proposed method is clearly better than the VF.

TABLE 1. Poles and residues of the TF of theoretical example

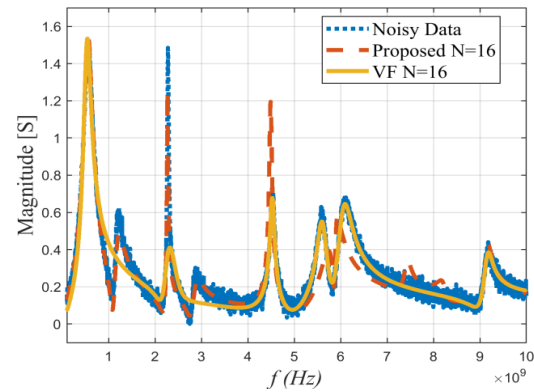| Poles (GHz)	Residues (GHz)
-0.6132±j3.4551	-0.9877±j0.0809
-0.3940±j7.3758	-0.2067±j0.0131
-0.0880±j14.3024	-0.1382±j0.0145
-0.4097±j17.7864	-0.1182±j0.0166
-0.2991±j28.4622	-0.2426±j0.0145
-0.6447±j35.2669	-0.4043±j0.0297
-1.0135±j37.9655	-0.6787±j0.1465
-0.5711±j57.4748	-0.2626±j0.1037
r_0=0.1	

Figure 6a. Magnitude of synthesized TF of theoretical example in the absence of noise

Figure 6b. Phase of synthesized TF of theoretical example in the absence of noise

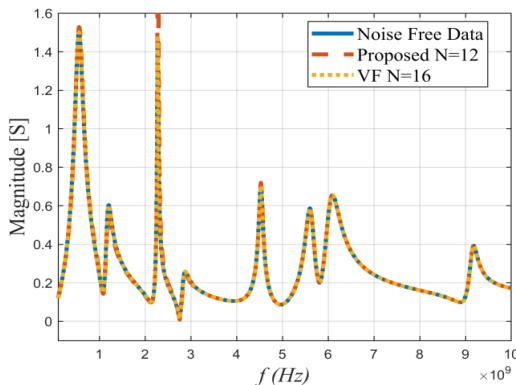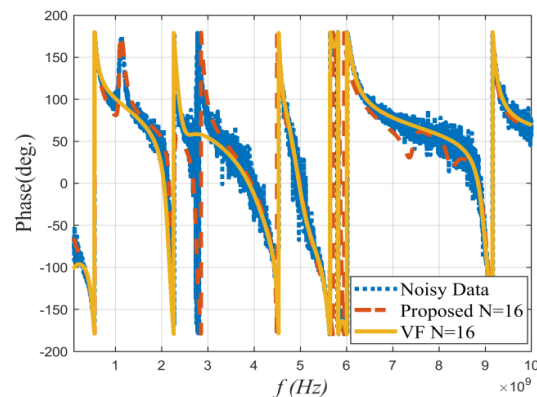**Figure 7a.** Magnitude of synthesized TF of theoretical example in the presence of noise

Figure 7b. Phase of synthesized TF of in the presence of noise

Now, consider the same transfer function in the presence of noise. Both real and imaginary parts of the transfer function are infected by white Gaussian noise. The noise level considered for this example is set to 20 dB signal-to-noise ratios (SNRs). The synthesized results of both VF and the proposed method with noisy data are depicted in Figure 7. Due to numerous fluctuations, it is not
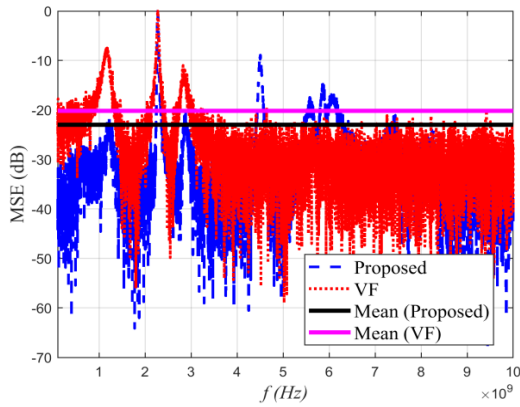
Figure 7c. Mean square error of TF vs. frequency for theoretical example

possible to compare the results from the figures correctly. For this reason, the diagram of the Mean Squares Error (MSE) in dB for both methods is also shown. It is observed that the proposed method has a lower MSE than VF, for about 2.8 dB averagely. In other words, the proposed method has more immunity with respect to noise. It should be noted that the noisy transfer function does not show smooth behavior and includes several sudden jumps versus frequency.

3. 4. Coupled Structure   The coupled structures are widely used in microwave engineering [32-33]. As the fourth example, a coupled microstrip line using TLY062 substrate with relative permittivity of 2.2, the thickness of 1.56 mm, and loss tangent 0.009 is considered [34]. The length and width of the board is 50 mm. The culprit and victim strip width are set to 4.8 mm, and the distance between two traces is about 0.5 mm. The measured far-end crosstalk is regarded as original data [34]. The fabricated of the understudying structure is shown in Figure 8 [34]. The magnitude and phase of rational approximation using the proposed method with N=9, 10, and vector fitting algorithm with N=14 poles are shown in Figure 9. It can be seen that the proposed method with N=9 shows a small deviation in magnitude in low frequencies. However, through increasing the poles number to N=10, the synthesized error is decreased. Although the accuracy of VF and the proposed method for N=10 is almost acceptable, the proposed method with a smaller number of poles shows better performance.
The relative error signals of all examples can be seen in Figures 10(a) to 10(c). It should be noted that the error signal of the third example (assumed TF with noise-infected data) is available in Figure 7c. It can be seen that in all examples except the second structure, the error value of the proposed method is lower than VF. Although in the second structure the error of VF is lower than the proposed method, the error value of the proposed method is less than 1%, and it is acceptable.
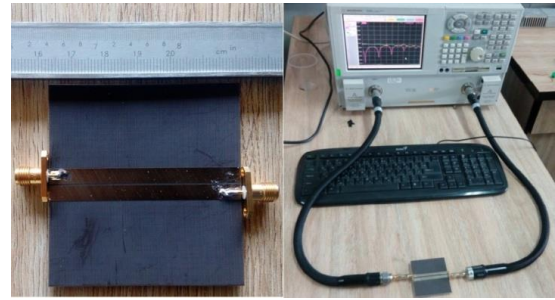

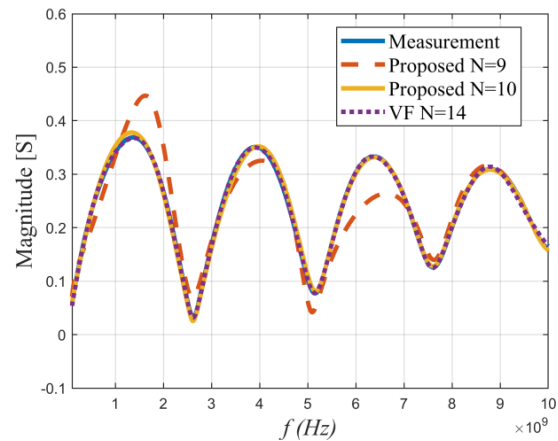**Figure 8.** The fabricated structure of coupled microstrip line [34]

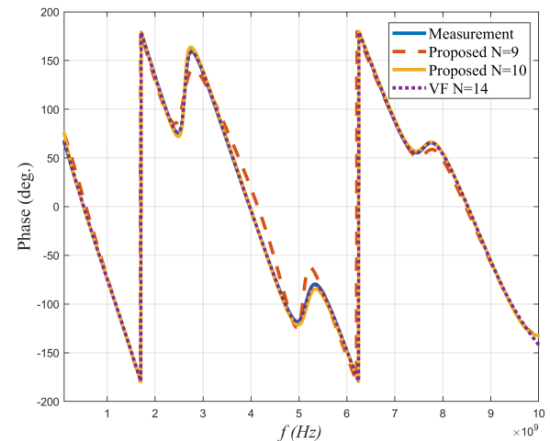**Figure 9a.** Magnitude of synthesized, far-end crosstalk of coupled microstrip line

Figure 9b. Phase of synthesized far-end crosstalk of coupled microstrip line

The condition numbers of coefficient matrix of Equations (5c) and (12c) (or (20a)) for all examples are reported in Table 2. It can be seen that the condition numbers of the coefficient matrix of Equations (5c) are very large in comparison to Equation (12c). Large condition numbers mean numerical difficulties in the
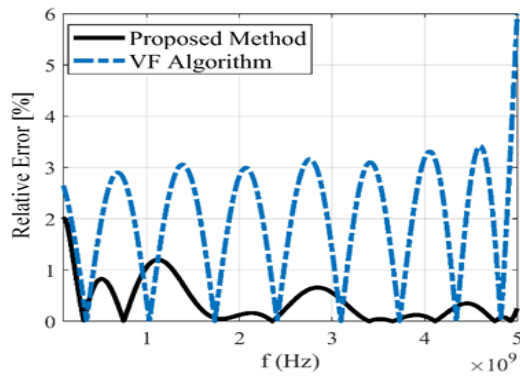
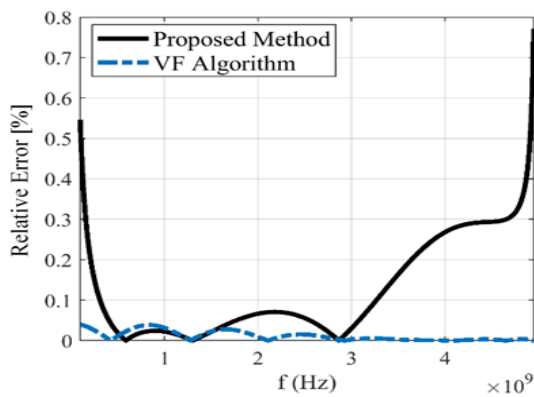**Figure 10a.** The relative error signal of single trace PCB

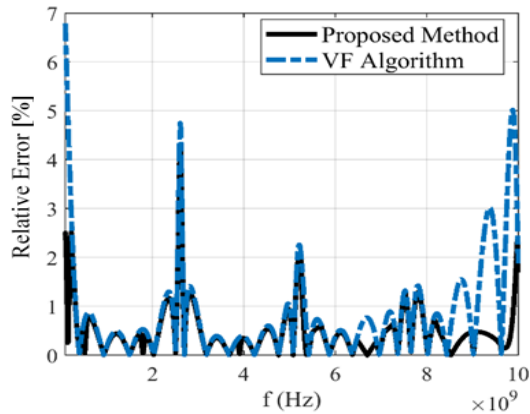**Figure 10b.** The relative error signal of multilayer structure

Figure 10c. The relative error signal of coupled structure

TABLE 2. Condition number of coefficients matrix for all examples

	N	Cond (5c)	Cond (12c) or (20a)
Example I	6	2.6542e+62	1.2724e+06
Example II	8	6.2741e+81	2.1412e+09
Example III	16	3.4643e+163	6.1996e+13
Example IV	10	9.6081e+103	3.4439e+09

4. CONCLUSION

In this paper, a mathematical method is presented to approximate the simulation or measurement data in the poles-residue form. The integration of the original data at several specified intervals, produces a system of linear equations that could be solved using the least square method. The stability condition of the provided model is guaranteed through defining a controller coefficient. To evaluate the performance of the proposed method, several practical examples were investigated and obtained results were compared with those obtained by the well-known vector fitting algorithm. The comparison showed that, in some cases, the proposed method could model the original data with a smaller number of poles than the VF algorithm. Also, the obtained results demonstrated that the performance of the method was less affected by noise. This is a very important point to notice since the measurement data is usually contaminated with noise.

5. ACKNOWLEDGMENTS

6. REFERENCES

1. Grivet-Talocia S, Gustavsen B, Passive Macromodeling: Theory and Applications. New York, NY, USA: Wiley, 2016.

2. Alijani M, G, H, Sheikh. S, Kishk. Ahmed, "Development of Closed-Form Formula for Quick Estimation of Antenna Factor", 15th European Conference on Antennas and Propagation (EuCAP), (2021), 1-5. doi: 10.23919/EuCAP51087.2021.9411008

3. Contreras. A, "Objective Functions for the Optimization of an Ultra Wideband Antenna", *International Journal of Engineering, Transaction A: Basics,* Vol. 34, No. 7, (2021), 1743-1749. doi: 10.5829/ije.2021.34.07a.19

4. Gupta. P, Pandey. R, "Dual Output Voltage Differencing Buffered Amplifier Based Active -C Multiphase Sinusoidal Oscillator", *International Journal of Engineering Transaction C: Aspects,* Vol. 34, No. 6, (2021), 1438-1444. doi: 10.5829/ije.2021.34.06c.07

5. Niasar. M, M, Molaei. M, J, Aghaei. A, "Electromagnetic Wave Absorption Properties of Barium Ferrite/Reduced Graphene

computation of the poles and residues of the final model [1]. Table 2 shows that the proposed method has created an extreme improvement in the condition number of coefficient matrix compared to the LSM method. This has led to a significant reduction in the computational error of the introduced method.

Oxide Nanocomposites", *International Journal of Engineering, Transaction C: Aspects*, Vol. 34, No. 6, (2021), 1503-1511. doi: 10.5829/ije.2021.34.06c.14

6. Yang. C, Bruns. H, D, Liu. P, Schuster. C, "Impulse response optimization of band-limited frequency data for hybrid field-circuit simulation of large-scale energy-selective diode grids", *IEEE Transaction Electromagnetic Compatibility*, Vol. 58, No. 4, (2016), 1072–1080. doi: 10.1109/TEMC.2016.2540921

7. Beygi. A, Time-domain macromodeling of high speed distributed networks. Ph.D. dissertation, The University of Western Ontario, 2011.

8. Alijani. M, G, H, Neshati. M, H, "A new non-iterative method for pattern synthesis of unequally spaced linear arrays", *International Journal of RF and Microwave Computer-Aided Engineering,* Vol. 29, No. 11, (2019), 740-771. doi: 10.1002/mmce.21921

9. Dounavis. A, Achar. R, Nakhla. M, S, "Addressing transient errors in passive macromodels of distributed transmission-line networks", *IEEE Transaction Microwave Theory Technique*, Vol. 50, No. 12, (2002), 2759-2768. doi: 10.1109/TMTT.2002.805130

10. Grivet-Talocia. S, Acquadro. S, Bandinu. M, Canavero. F, G, Kelander. I, Rouvala. M, "A parameterization scheme for lossy transmission line macromodels with application to high speed interconnects in mobile devices", *IEEE Transaction Electromagnetic Compatibility*, Vol. 49, No. 1, (2007), 18-24. doi: 10.1109/TEMC.2006.888179

11. Ferranti. F, Knockaert. L, Dhaene. T, "Guaranteed passive parameterized admittance-based macromodeling", *IEEE Transaction on Advanced Packaging*, Vol. 33, No. 3, (2010), 623-629. doi: 10.1109/TADVP.2009.2029242

12. Gustavsen. B, Semlyen. A, "Rational approximation of frequency domain responses by vector fitting", *IEEE Transactions on Power Delivery,* Vol. 14, No. 3, (1999), 1052-1061. doi: 10.1109/61.772353

13. Deschrijver. D, Mrozowski. M, Dhaene. T, De-Zutter. D, "Macromodeling of multiport systems using a fast implementation of the vector fitting method", *IEEE Microwave Wireless Component Letter*, Vol. 18, No. 6, (2008), 383-385. doi: 10.1109/LMWC.2008.922585

14. Dhaene. T, De-Zutter. D, "Selection of lumped element models for coupled lossy transmission lines", *IEEE Transaction Computer-Aided Design Integrated Circuits System*, Vol. 11, No. 7, (1992), 805-815. doi: 10.1109/43.144845

15. Kabir. M, Khazaka. R, "Macromodeling of distributed networks from frequency domain data using the Loewner matrix approach", *IEEE Transaction Microwave Theory Technique*, Vol. 60, No. 12, (2012), 3927-3938. doi: 10.1109/TMTT.2012.2222915

16. Rergis. C, M, Kamwa. I, Khazaka. R, Messina. A, R, "A Loewner Interpolation Method for Power System Identification and Order Reduction", *IEEE Transactions on Power Systems*, Vol. 34, No. 3, (2019), 1834-1844. doi: 10.1109/TPWRS.2018.2884655

17. Odabasioglu. A, Celik. M, Pileggi. L, T, "PRIMA: passive reduced-order interconnect macromodeling algorithm", *IEEE Transaction Computer-Aided Design Integrated Circuits System,* Vol. 17, No. 8, (1998), 645-654. doi: 10.1109/43.712097

18. Dounavis. A, Achar. R, Nakhla. M, S, "Efficient passive circuit models for distributed networks with frequency-dependent parameters", *IEEE Transaction Advanced Packaging*, Vol. 23, No. 3, (2000), 382-392. doi: 10.1109/6040.861551

19. Dounavis. A, Achar. R, Nakhla. M, "A general class of passive macromodels for lossy multi-conductor transmission lines", *IEEE Transaction Microwave Theory Technique*, Vol. 49, No. 10, (2001), 1686-1696. doi: 10.1109/22.954772

20. Cangellaris. A, C, Pasha. S, Prince. J, L, Celik. M, "A new discrete transmission line model for passive model order reduction and macromodeling of high-speed interconnections", *IEEE Transaction Advanced Packaging,* Vol. 22, No. 3, (1999), 356-364. doi: 10.1109/6040.784485

21. Yu. Q, Wang. J, M, L, Kuh. E, S, "Passive multipoint moment matching model order reduction algorithm on multiport distributed interconnect networks", *IEEE Transaction Circuits System I: Fundamental Theory and Applications*, Vol. 46, No. 1, (1999), 140-160. doi: 10.1109/81.739262

22. Gad. E Nakhla. M, "Efficient simulation of non-uniform transmission lines using integrated congruence transform", *IEEE Transactions on Very Large Scale Integration (VLSI) Systems,* Vol. 12, No. 12, (2004), 1307-1320. doi: 10.1109/TVLSI.2004.837988

23. Lefteriu. S, Antoulas. A, C, "A new approach to modelling multiport systems from frequency-domain data", *IEEE Transactions Computed-Aided Design Integrated Circuits System*, Vol. 29, No. 1, (2010), 14-27. doi: 10.1109/TCAD.2009.2034500

24. Alijani. M, G, H, Neshati. M, H, "A New Closed-Form Expression for Dispersion Characteristics of Fundamental Mode of SIW by Least Squares Method", *Journal of Applied Computational Electromagnetic Society*, Vol. 30, No. 8, (2015), 930-933.

25. Mendel. J, M, Lessons in Estimation Theory for Signal Processing, Communications, and Control. Prentice Hall PTR, 1995.

26. Alijani. M, G, H, Neshati. M, H, "Development a New Technique Based on Least Square Method to Synthesize the Pattern of Equally Space Linear", *International Journal of Engineering, Transaction B: Applications,* Vol. 32, No. 11, (2019), 1620-1626. doi: 10.5829/ije.2019.32.11b.13

27. Alijani. M, G, H, Neshati. M, H, "Development A New Array Factor Synthesizing Technique by Pattern Integration and Least Square Method", *IEEE Transaction Antennas and Propagation*, Vol. 66, No. 12, (2018), 6869-6874. doi: 10.1109/TAP.2018.2871715

28. Courant. R, Hilbert. D, Methods of Mathematical Physics. John Wiley & Sons, 1989.

29. Pan. V, Y, "Solving a Polynomial Equation: Some History and Recent Progress", *SIAM Review,* Vol. 39, No. 2, (1997), 187-220. doi: 10.1137/S0036144595288554

30. Beygi. A, Dounavis. A, "An instrumental variable vector-fitting approach for noisy frequency responses", *IEEE Transaction Microwave Theory Technique*, Vol. 60, No. 9, (2012), 2702-2712. doi: 10.1109/TMTT.2012.2206399

31. http://www.energy.sintef.no/Produkt/VECTFIT/index.asp.

32. Rashtian. M, Vafapour. M, "Gain Boosted Folded Cascade Op-Amp with Capacitor Coupled Auxiliary Amplifiers", *International Journal of Engineering, Transaction B: Applications,* Vol. 34, No. 5, (2021), 1233-1238. doi: 10.5829/ije.2021.34.05b.16

33. Sobouti. M, A, Azizian. D, Bigdeli. M, Gharehpetian. G, B, "Multi-Conductor Transmission Line Model of Split-Winding Transformer for Frequency Response and Disk-to-Disk Fault Analysis", *International Journal of Engineering, Transaction C: Aspects* Vol. 34, No. 6, (2021), 1486-1492. doi: 10.5829/ije.2021.34.06c.12

34. Soleimani. N, Alijani. M, G, H, Neshati. M, H, "Crosstalk Analysis of Multi-Microstrip Coupled Lines Using Transmission Line Modeling", *International Journal of RF and Microwave Computer-Aided Engineering*, Vol. 22, No. 6, (2019), 1-7. doi: 10.1002/mmce.21677

Persian Abstract

چکیده

در این مقاله ، یک روش جدید برای سنتز داده های به دست آمده از نتایج شبیه سازی یا اندازه گیری در قالب یک تابع کسری معرفی شده است. انتگرال گیری از داده های موجود نقش مهمی در عملکرد روش پیشنهادی دارد. مقادیر قطب ها و مانده های مدل کسری با حل سیستم معادلات خطی با روش حداقل مربعات (LSM) تعیین می شود. برای اطمینان از شرایط پایداری مدل ارائه شده، ضریب کنترل کننده در نظر گرفته شده است. همچنین، با استفاده از این پارامتر، طراح می تواند حاشیه پایداری سیستم را با شرایط پایداری ضعیف افزایش دهد. روش معرفی شده امکان استفاده در طیف گسترده ای از کاربردهای عملی را فراهم می کند زیرا محدودیت خاصی در استفاده از این روش وجود ندارد. تنها موردی که باید در نظر گرفته شود شرط دیریچله برای داده های اصلی است که معمولاً در مورد سیستم های فیزیکی برقرار است. برای تأیید عملکرد روش پیشنهادی، چندین مورد مثال کاربردی بررسی شده و نتایج بدست آمده با نتایج بدست آمده توسط الگوریتم برازش برداری مقایسه می شود. همچنین، نتایج شبیه سازی نشان می دهد که این روش در حضور داده های نویزی کارآمد است.